

Redox-Active Dihydrazone and its Manganese(IV) Complexes: Synthesis, Characterization, Electrochemical and Antimicrobial Studies

Mahanta P.¹, Sarma P.¹, Basumatary D.^{1*} and Medhi C.²

1. Department of Applied Sciences, Chemical Science Division, Gauhati University, Guwahati, Assam, INDIA

2. Department of Chemistry, Gauhati University, Guwahati, Assam, INDIA

*debbasumatary@gauhati.ac.in; debbasumatary@gmail.com

Abstract

The +4 oxidation state of manganese has sparsely been documented so far. Few studies have reported deriving the high valent state of metals from dihydrazones. In this study, the synthesis and structure elucidation coupled with the study of electron transfer and biological properties of the polyfunctional ligand, bis(2-hydroxy-1-naphthaldehyde)fumaryl dihydrazone (napfhH₄) and its manganese(IV) complexes ([Mn^{IV}(napfh)](A)₂·2H₂O and [Mn^{IV}(napfh)(NN)]), where A = H₂O, (1); pyridine, (py, 2); 2-picoline, (2-pic, 3); 3-picoline, (3-pic, 4); 4-picoline, (4-pic, 5) and NN = 2, 2'-bipyridine, (bpy, 6) and 1, 10-phenanthroline, (phen, 7)) were undertaken. IR spectral studies revealed that napfhH₄ coordinates to manganese center in a tetradentate manner arranged in anti-cis configurations in these complexes and in keto-enol form in the complexes (1), (2), (6) and (7) while in complexes (3)-(5), it exists in keto form.

The magnetic moment, electronic and electron paramagnetic resonance spectral studies corresponded to Mn(IV) center within six-coordinate octahedral geometry around the manganese center. Molar conductances in DMSO indicated their non-electrolytic nature. The redox activity of the ligand and one electron transfer of Mn(IV)/Mn(III) in complexes were evaluated. Further, the increased antimicrobial efficacies against different pathogenic gram-positive and gram-negative bacteria suggest these complexes as good candidates for other biological studies such as antitumour activity.

Keywords: Manganese(IV), Bis(2-hydroxy-1-naphthaldehyde)fumaryl dihydrazone, Pyridine bases, Redox-activity, Antimicrobial activity.

Introduction

In nature, the high-valent manganese gives impetus to several biological processes¹³. It serves to supply electrons for O₂ evolution from water oxidation during green plant photosynthesis¹⁸ and promotes superoxide dismutase⁶, arginase² and catalase²⁷ activity. Notably, the high-valent manganese in O, N donor sites of synthetic complexes is well known to be good candidate as biomimetic model for

* Author for Correspondence

biological systems²⁷. Further, Mn (IV) oxides were established in many reports to facilitate abiotic humification in the environment better than any other metal oxides due to their high reduction potentials and mixed-valence configurations³⁴. Also, they are known to play a pivotal role in many synthetic processes^{2,11,28,33} and as large molecular magnets³³. Incidentally, the higher valent manganese complexes have sparsely been documented so far^{27,29}.

Many studies have reported that the dihydrazones are electron-rich systems^{8,11,12} and are redox-active chelates¹¹. Literature records and many of our studies on transition metal complexes of dihydrazones have shown that these polychelates have the potential to stabilize the high oxidation state of metals^{2,11,12}. In continuation of our work on manganese complexes of dihydrazones, we intended to synthesize high valent manganese complexes, so it was of our pertinent interest to synthesize and study these complexes.

The ligand, bis(2-hydroxy-1-naphthaldehyde)fumaryl dihydrazone (napfhH₄) was selected in this study. The condensation of an o-hydroxy aromatic aldehyde with an acylhydrazine has formed the dihydrazone, napfhH₄ which contains two identical moieties of secondary amido (R-CO-NH-), azomethine (-C=N-) and o-hydroxy (-OH) functional groups in its molecular skeleton^{11,26}. Such bulky polynucleating chelates have tremendous potential of discrete structural variability and accessibility to different oxidation states of metals on coordination^{2,29,30}. The dihydrazones may yield mononuclear or polynuclear complexes that can exist in keto, enol or keto-enol form having discrete molecularity¹⁵.

Another facet of this study is that the N₂O₂ donor, core of the dihydrazones provide a simple mechanistic model to support the closely related biological systems⁹. Numerous studies have attributed their biological and chemical properties that pertain to their wide applications in areas like inorganic, organic, medicinal and analytical chemistry to the presence of -NC=O and -C=NH moieties in their structure^{3,15}.

In the present study, the monodentate and bidentate pyridine bases were also incorporated as secondary ligands. Pyridine and its derivatives are found in alkaloids, enzymes and many such biological molecules and so have the promising potential of applications in the pharmaceutical industry⁵.

Thus, the work carried out aimed to synthesize, characterize, study the redox behaviour and screen the antimicrobial activity of the manganese(IV) complexes derived from bis(2-hydroxy-1-naphthaldehyde)fumaryldihydrazone.

Material and Methods

Materials: The chemicals $Mn(OAc)_2 \cdot 4H_2O$, hydrazine hydrate ($N_2H_4 \cdot H_2O$), salicylaldehyde, diethyl fumarate ($C_2H_5OCOCH=CHCOOC_2H_5$), ethanol and methanol were of analytical grade reagents.

Physical measurements: Standard procedure was followed to determine manganese³². Metal complexes in DMSO ($\sim 10^{-3}$ M) were prepared and their molar conductances were measured using direct reading conductivity meter-304 with a dip-type conductivity cell at room temperature. Magnetic susceptibilities were measured on a Sherwood Scientific Magnetic Susceptibility Balance with $Hg[Co(SCN)_4]$ as the calibrating agent at room temperature. Infrared (IR) spectral data were obtained using Spectrum 2 Perkin-Elmer FTIR spectrometer from 500-4000 cm^{-1} in KBr disks. EPR spectral data of the complexes as powders and in DMSO were measured on the JES-FA200 ESR spectrometer with X-band frequency at room temperature (RT) and liquid nitrogen temperature (LNT). ESI-MS spectrum was obtained from UHPLC-ULTIMATE 3000, Thermo scientific, MS-Exactive Plus spectrometer.

Electronic spectral data were obtained within the range 250 to 800 nm in DMSO on a Perkin-Elmer Lambda 35 UV-Vis spectrophotometer. Melting point and decomposition temperatures were obtained using the Analab melting apparatus, μ Thermocal 10. Thermal analysis of the complexes was studied as representative cases by using Mettler Toledo thermal analyzer system recording TGA and DTG curves within the temperature range 25-700 °C under the nitrogen atmosphere at a heating rate of 20 °C/min. Electrochemical studies for complexes in DMSO were carried under pure and dry dinitrogen atmosphere using CHI660D CH INSTRUMENT electrochemical work station with Pt disk as a working electrode, a Pt wire auxiliary electrode and Ag/AgCl reference electrode.

Synthesis of napfhH₄: The ligand, bis(2-hydroxy-1-naphthaldehyde)fumaryldihydrazone (napfhH₄) was prepared in two steps. In the first step, fumaric hydrazide was prepared by reacting diethyl fumarate (3.40 g, 19.75 mmol) and hydrazine hydrate (1.90 g, 39.50 mmol) in 1:2 molar ratios. In the second step, fumaric dihydrazide thus obtained was allowed to react with 2-hydroxy-1-naphthaldehyde (1.45 g, 8.42 mmol) in 1:2 molar ratios by refluxing for 1 hour in methanol. A yellow precipitate was obtained that was washed several times with hot methanol and dried over anhydrous $CaCl_2$ (D.P >250 °C).

Synthesis of $[Mn^{IV}(napfh)(H_2O)] \cdot 2H_2O$ (1): $Mn(OAc)_2 \cdot 4H_2O$ (0.22g, 1 mmol) in methanol (15 ml) was added to a methanolic solution of ligand (napfhH₄) (0.38 g,

1 mmol) at 1:1 molar ratio. This reaction mixture was stirred at room temperature for 30 minutes and then refluxed for 2 hrs. This precipitated a reddish-brown compound that was filtered hot, washed with hot methanol several times and finally dried over anhydrous $CaCl_2$, (Yield: 65%).

Synthesis of $[Mn^{IV}(napfh)(A)_2] \cdot 2H_2O$ (2)-(5): The compounds $[Mn^{IV}(napfh)(A)_2] \cdot 2H_2O$ (A= pyridine (py, 2); 2-picoline (2-pic, 3); 3-picoline (3-pic, 4) and 4-picoline (4-pic, 5) were prepared by essentially following the above procedure except that the pyridine bases were also simultaneously added to the solution mixture of $Mn(OAc)_2 \cdot 4H_2O$ and ligand in the molar ratio 1:1:10 of $Mn(OAc)_2 \cdot 4H_2O$: ligand: pyridine bases. The reddish-brown and brick red coloured compounds obtained were isolated by filtering and washing several times with methanol and dried over $CaCl_2$, [Yield (2), (3) = 62%; (4), (5) = 63 %].

Synthesis of $[Mn^{IV}(napfh)(NN)]$ (6) and (7): The compounds $[Mn^{IV}(napfh)(NN)]$ (where NN = 2, 2 bipyridine (bpy, 6) and 1, 10-phenanthroline (phen, 7)) were prepared by following the above essential procedure except that the bipyridine and 1, 10 phenanthroline bases were also added to $Mn(OAc)_2 \cdot 4H_2O$ and ligand solution mixture in the molar ratio of 1:1:2 in methanol. The brick-red coloured compounds obtained were isolated by filtering and washing with methanol and dried over $CaCl_2$ [Yield (6) = 64%; (7) = 67 %].

Antimicrobial susceptibility tests: The *in vitro* antibacterial properties of the uncoordinated ligand and its manganese complexes (1)-(5) were screened against the gram-positive bacteria-*Staphylococcus epidermis* (MTCC 435), *Bacillus cereus* (MTCC 1305) and gram-negative bacteria-*Klebsiella pneumonia* (MTCC 10309), *Escherichia coli* (MTCC 1669), *Enterobacter aerogenes* (MTCC 8559) and *Proteus vulgaris* (MTCC 426). The standard agar well diffusion method was followed for studying the antimicrobial activities²⁵.

In this method the ligand and complexes (1) - (5) that were used as test compounds were allowed to diffuse through an agar gel previously inoculated with a test bacterial pathogen. After incubation of the plates for 24-48h, the bacterial colonies showed growth wherever it was possible and also produced a haze in the agar. The solvent (dilute DMSO) used for test compounds was also tested as the negative control to ascertain that the antimicrobial activity was not due to the solvent.

Results and Discussion

The complexes are stable in air and non-hygroscopic. They are found to be insoluble in water and common organic solvents like acetone, ethanol, methanol etc. However, they are completely soluble in solvents like dimethyl sulphoxide (DMSO) and dimethylformamide (DMF). Their insolubility in most solvents has rendered their inability to crystallize by

different methods in several attempts and has only produced degraded solid compounds.

The characterization data for complexes with their elemental analysis, colour, decomposition point (D.P.), magnetic moment and molar conductance are presented in table 1.

Thermal studies: The complexes do not decompose or melt up to the observed temperature range of 250 °C that reveals strong metal-ligand bonds with higher ionic character. The complexes (1)-(3) were studied as representative samples by thermogravimetric analysis. The TGA/DTG curve of

complex (1) exhibited degradation within the temperature range of 26-135 °C with a DTG peak at 66 °C. The corresponding weight loss of 8.2% (calcd. 6.3%) was suggested to be due to the weight loss of two lattice water molecules. The second stage degradation within the temperature range of 135-285 °C with DTG peak at 226 °C and weight loss of 5.16% (calcd. 6.3%) corresponds to the liberation of two coordinated water molecules.

Details for the stages of thermal decomposition and the percentage loss of masses along with their assigned molecules/fragments are summarized in table 2.

Table 1
Colour, decomposition point, molar conductance for monometallic manganese (IV) of dihydrazone

Complex	Colour	D.P (°C)	Analysis: Found (calcd.)%	μ_B (B.M)	Molar conductance (Λ_m) ($\text{ohm}^{-1}\text{cm}^2 \text{mol}^{-1}$)
			Mn		
[Mn ^{IV} (napfh)(H ₂ O) ₂].2H ₂ O (1)	Reddish brown	>250	9.10 (9.55)	3.52	1.5
[Mn ^{IV} (napfh)(py) ₂].2H ₂ O (2)	Reddish brown	>250	6.94 (7.53)	3.77	1.9
[Mn ^{IV} (napfh)(2-pic) ₂].2H ₂ O (3)	Reddish brown	>250	7.21 (7.55)	3.82	2.5
[Mn ^{IV} (napfh)(3-pic) ₂].2H ₂ O (4)	Reddish brown	>250	7.68 (7.55)	4.1	2.8
[Mn ^{IV} (napfh)(4-pic) ₂].2H ₂ O (5)	Brick red	>250	7.11 (7.55)	4.21	1.5
[Mn ^{IV} (napfh)(bpy)] (6)	Brick red	>250	7.50 (8.33)	3.44	2.2
[Mn ^{IV} (napfh)(phen)] (7)	Brick red	>250	8.01 (8.33)	3.91	2.7

Table 2
Thermoanalytical results (TG and DTG) of manganese(IV) complexes of napfhH₄

Complexes	TG range (°C)	DT G (°C)	Found (calcd. %)		Assignment
			Mass loss	Total mass loss	
[Mn ^{IV} (napfh)(H ₂ O) ₂].2H ₂ O (1)	26-135 135-285 285-328 328-375 375-428 499-609	66 226 301 352 392 551	8.2(6.3) 5.16(6.3) 12.42(11.8) 23.71(23.26) 31.87(31.60) 4.59(5.9)	87.65(85.16)	Loss of two lattice H ₂ O molecules Loss of two coordinated H ₂ O molecules Loss of organic moiety (CHCON ₂) Loss of organic moiety (CHCON ₂ C ₅ H ₆) Loss of organic moiety (C ₁₁ H ₉ ON ₂) Loss of two OH molecules
[Mn ^{IV} (napfh)(py) ₂].2H ₂ O (2)	35-145 145-275 275-329 329-383 383-490 490-610	61 225 321 355 397 566	3.84(5.15) 2.93(2.29) 12.25(11.8) 25.6(26.39) 17.37(16.62) 6.75(7.74)	68.74(69.99)	Loss of two lattice H ₂ O molecule Loss of NH ₂ Loss of organic moiety (CHCON ₂) Loss of two pyridine molecules & C ₂ H ₂ Loss of two organic moieties (CON ₂ H ₂) Loss of C ₂ H ₂ N ₂
[Mn ^{IV} (napfh)(2-pic) ₂].2H ₂ O (3)	31-118 118-276 276-324 324-380 380-439	71 229 312 353 394	4.94(4.96) 2.4(2.20) 14.03(13.35) 29.85(29.23) 8.96(7.45)	60.18(59.32)	Loss of two lattice H ₂ O molecules Loss of NH ₂ Loss of organic moiety (CHCON ₂) & C ₂ H ₂ Loss of two 2-picoline molecules & C ₂ H ₂ Loss of C ₂ H ₂ N ₂

These thermal investigations indicated the presence of two water molecules in the lattice of complexes (1) - (3) and also two coordinated water molecules in the structure of complex (1) which are in good agreement with their IR spectral studies.

Molar conductance: The complexes have molar conductance value within the range 1.5-2.8 ohm⁻¹cm²mol⁻¹ in DMSO solution (table 1) that indicate their non-electrolytic nature in this solvent^{7,11,29}.

Magnetic moment: The μ_B values for Mn(IV) complexes reported here lie in the range 3.44-4.21 B.M (table 1) suggesting the presence of d³ configuration (S=3/2) in octahedral geometry ruling out the possibility of any spin-spin coupling in the solid-state between unpaired electrons belonging to different Mn(IV) centers in the structural unit of the complexes^{2,11,29}.

Mass spectrum: The complex (3) was studied by ESI-MS spectroscopy as a representative sample. The fragmentation peak observed at m/z = 556.4024 in the mass spectrum of the complex is attributed to its cleavage and may have resulted from the formation of the fragmented species of [Mn(napfh-C₃H₃N)]⁺. Another intense signal at m/z = 570.4184 is probably due to the formation of [Mn(napfh-C₄H₅N)]⁺ species. These signals in the mass spectrum of different chemical species are indicative of the composition of this complex and its monomeric nature.

Electronic spectra: The absorption spectrum of the free ligand is characterized by the absorption bands at 287(3264), 292(1398), 294(3053), 320(4095), 332(5155) 380(6505) and 472(666) nm (table 3). The band at 380 nm is reported to be a characteristic feature of naphthalaldimine moiety^{17,22,29} and the band at 472 nm is correlated with the forbidden transition

in dihydrazone²⁹. The intra-ligand bands between 287-294 nm are assigned to arise from π - π^* and those between 320-380 nm are attributed to n- π^* transitions.

The complexes display similar absorptions to that observed in the ligand with no shifts or small shifts in the position of bands between the region 287-380 nm; they however exhibited hyperchromic effects with a large increase in intensities of bands, so they are most likely to occur due to transitions involving the ligand orbitals only. Likewise, the complexes also exhibit a band at 472 or 475 nm. The high molar extinction coefficient of this band at 472 or 475 nm with no shift or small redshift by 3 nm in band position in the complexes may be attributed to ligand centered band with contributions from charge transfer transitions. In complexes (3)-(7), an additional band at 448 or 452 nm is observed.

In complexes (3)-(7), an additional band at 448 or 452 nm is observed. The large intensity of this band may be attributed to charge-transfer between the ligand and the metal center. The complexes (6) and (7) possess another band at 503 nm that is attributed to d-d transitions of the Mn(IV) center with contribution from the charge transfer band due to its reasonably high molar extinction coefficient value unexpected from bands due to d-d transitions only^{11,16,29}.

Octahedral Mn(IV) complexes are usually expected to show three spin allowed d-d transitions which are $^4A_{2g} \rightarrow ^4T_{2g}$, $^4A_{2g} \rightarrow ^4T_{1g}(F)$ and $^4A_{2g} \rightarrow ^4T_{1g}(P)$ ^{11,30}. In correlation with the works reported by Kessissoglou at al¹⁰ and Okawa at al²¹, it is suggested that the band at 503 nm in the complexes (6) and (7) may be attributed to d-d transition, $^4A_{2g} \rightarrow ^4T_{2g}(F)$. Thus, these electronic spectral features of the complexes indicate strong chelation of the dihydrazone to the manganese center.

Table 3
Important electronic spectral bands and EPR data for manganese(IV) complexes

Ligand/ complex	$\lambda_{max}(nm)$ ($\epsilon_{max} M^{-1} cm^{-1}$) for conc. $10^{-4} M$ soln	Temp	solid/soln	g-value	$A_{Mn}(G)$
napfhH ₄	287(3264), 292(1389), 294(3053), 320(4095), 332(5155), 380(6505), 472(666)				
1.	287(4758), 292(4479), 294(4200), 321(4407), 333(4949), 369(5280), 472(3284)	RT	DMSO	1.990	91.80
		LNT	DMSO	1.997	95.64
2.	287(3735), 292(4058), 294(4045), 321(4019), 333(4419), 366(4674), 472(3074)	RT	DMSO	1.993	92.95
		LNT	DMSO	1.928	90.88
3.	287(3393), 291(3390), 295(3312), 319(4182), 332(3983), 372(4455), 448(1944)sh, 472(2073)				
4.	287(3683), 292(2810), 294(3792), 319(3928), 332(4656), 375(5384), 448(1675), 475(1636)				
5.	- 293(5090) - 319(6131), 333(7509), 374(8263), 448(2750), 472(2671)				
6.	287(3065), 289(2853), 292(2666), 318(3273), 333(4110), 376(4650), 452(935), 475(919), 503(650)	LNT	DMSO	1.984	96.52
		RT	DMSO	1.998	92.61
7.	287(3760), 291(4079), 294(4025), 320(5466), 333(7015), 376(8263), 452(1191), 475(1160), 503(687)				

EPR spectra: The complexes (1), (2) and (6) were studied by EPR spectroscopy at LNT and RT in DMSO as representative samples (table 3). At LNT, the complexes in DMSO exhibited similar spectral features displaying isotropic signal and superhyperfine lines. Likewise, at RT, the complexes exhibited similar spectral features in DMSO with six hyperfine lines.

The ^{55}Mn hyperfine splitting constant for these complexes at LNT and RT falls in the range of 90.88–96.52 G with g value in the range of 1.928–1.998. The Mn hyperfine splitting constant is characteristic of Mn(IV) complexes for d^3 ion rather than for Mn(II) complexes^{11,29}. The zero-field splitting parameters are used to describe the magnetostructural properties for transition metal complexes with $S > 1/2$. These Mn(IV) complexes display an isotropic metallic center with a strong signal at $g \approx 2$ due to spatially nondegenerate $^4A_{2g}$ ground term that affirms an octahedral symmetry of Mn(IV) mononuclear species with $D=0$ ^{23,33}.

Infrared spectra: The IR spectra of free dihydrazone, complexes (1), (3) and (6) are presented in fig. 1. The ligand shows a strong and sharp band at 3337 cm^{-1} that is attributed to νOH while another strong and sharp signal at 3256 cm^{-1} is assigned to νNH ^{11,29} (table 4). The dihydrazone exhibits a strong band of $\nu(\text{C}=\text{O})$ at 1657 cm^{-1} . The appearance of νNH

and $\nu(\text{C}=\text{O})$ concurrent bands indicates that the ligand exists in keto form^{11,29}.

The strong couple of bands at 1624 (s) and 1598 (s) is attributed to $\nu(\text{C}=\text{N})$ ^{24,31} that indicates the presence of the free ligand in anti-cis configuration^{11,29}. In such a situation, one hydrazone arm of the dihydrazone is present axially and relatively absorbs at a lower frequency compared to the other (equatorial). The bands at 1538 (s) ; 1283 (m) and 1018 (s) in free ligands are attributed to $\nu(\text{Amide-II})$, $\nu(\text{C-O})$ (naphtholic); $\beta(\text{C-O})$ (naphtholic) and $\nu(\text{N-N})$ respectively^{11,29,24,31}.

Notably, the peak to peak comparisons of the spectrum of the ligand with those of complexes showed that the complexes (1), (2), (6) and (7) exhibit almost no shift of the bands with their intensities reduced to almost half. It is noted that the shape of spectral bands of complexes (1) and (2) is very similar to the ligand. Meanwhile, the infrared spectral shape of complexes (6) and (7) are similar to the ligand and also to one another but are significantly subdued. The appearance of un-shifted $\nu(\text{OH}+\text{NH})$, $\nu(\text{C}=\text{O})$, $\nu(\text{N-N})$ and $\nu(\text{Amide-II}) + \nu(\text{C-O})$ (naphtholic) bands in complexes (1), (2), (6) and (7) with reduced intensities may indicate that half of the ligand molecule retained the keto form or in other words, the existence of keto-enol form.

Table 4
Structurally significant IR spectral bands of ligand and its monometallic manganese(IV) complexes

Ligand/Complex	$\nu(\text{OH})+\nu(\text{NH})$	$\nu(\text{C}=\text{O})$	$\nu(\text{C}=\text{N})$	Amide(II)+ $\nu(\text{CO})$ naphtholic	$\beta(\text{C-O})$ (naphtholic)	$\nu(\text{N-N})$	$\nu(\text{M-O})$ naphtholic	$\nu(\text{M-N})$ py/bpy/phen vibration in plane
napfhH ₄	3337(s) 3256(s)	1657(s)	1624(s) 1598(s)	1538(s)	1283(m)	1018(s)	-	-
1	3000-3600(sbr) 3435(sbr) 3338(s) 3256(s)	1657(s)	1617(s) 1598(s)	1537(s)	1283(w) 1300(m)	1018(s)	512(w) 582(w)	-
2	3000-3600(sbr) 3432(sbr) 3338(m) 3256(m)	1657(s)	1617(s) 1598(s)	1537(s)	1283(w) 1300(w)	1018(s)	513(w) 582(w)	696(m)
3	3000-3600(sbr) 3443(sbr)	1655(s)	1624(s) 1597(s)	1537(s)	1283(w) 1300(w)	1018(m)	533(w) 554(w)	619(w) 646(w)
4	3000-3600(sbr) 3449(sbr)	1656(s)	1625(s) 1601(s)	1537(s)	1283(w) 1300(w)	1017(m)	532(m) 554(w)	616(w) 650(w)
5	3000-3600(sbr) 3443(sbr)	1657(s)	1625(s) 1601(s)	1537(s)	1283(m) 1300(w)	1017(m)	532(m) 554(w)	619(w) 649(w)
6	3337(m) 3256(m)	1658(s)	1626(s) 1598(s)	1537(m)	1283(m)	1017(m)	532(w) 554(w)	697(s)
7	3338(m) 3257(m)	1658(s)	1627(s) 1598(s)	1538(s)	1283(m)	1018(m)	532(w) 552(w)	699(m)

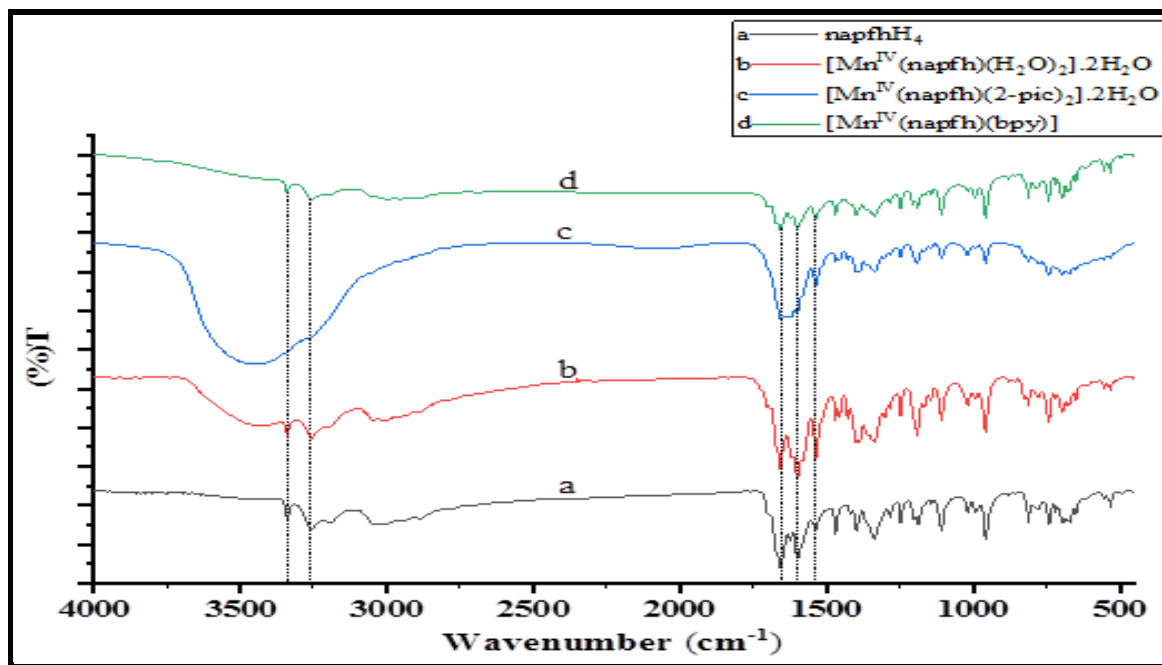


Fig. 1: IR spectra of (a) ligand naphH_4 and complexes (b) $[\text{Mn}^{\text{IV}}(\text{naphH})(\text{H}_2\text{O})_2] \cdot 2\text{H}_2\text{O}$ (2) (c) $[\text{Mn}^{\text{IV}}(\text{naphH})(2\text{-pic})_2] \cdot 2\text{H}_2\text{O}$ (3) (d) $[\text{Mn}^{\text{IV}}(\text{naphH})(\text{bpy})]$ (6)

The reduced intensities and un-shifted positions of these bands in these complexes also dismiss the possibility of involvement of twin donors of $-\text{OH}$, $-\text{NH}$, $>\text{C}=\text{O}$ and $>\text{C}=\text{N}$ groups and hence their association in coordination to the metal center may be partly. The $\beta(\text{C}-\text{O})$ (naphtholic) at 1283 cm^{-1} in the ligand undergoes splitting into two weak bands at 1283 and 1300 cm^{-1} in complexes (1) and (2) which also have reduced intensities that appear to be the effect of bonding of one of the naphtholic $\text{C}-\text{O}$ group to the metal center^{11,24,29,31} while it remains as a single un-shifted band in complexes (6) and (7).

Likewise, the un-shifted position of one of the couple of $\nu(\text{C}=\text{N})$ bands suggests that one bond is coordinated and the other remains free as depicted by the presence of one un-shifted band position at 1598 cm^{-1} and the other band is shifted in the region between $1617\text{-}1627 \text{ cm}^{-1}$ in the complexes. The $\nu(\text{N}-\text{N})$ band appears weak in IR spectra of the complexes (1), (2), (6) and (7) and retains almost the same positions as in free ligand, indicating bonding of only one hydrazinic nitrogen to the metal.

In complexes (3) - (5), the disappearance of νOH and νNH bands indicates the absence of $-\text{OH}$ and $-\text{NH}$ groups and suggests their involvement in complexation to the metal center. Almost similar band position of $\nu(\text{C}=\text{O})$ as that of the ligand rules out its involvement in coordination to the metal center and indicates the existence of keto form of the dihydrazone in complexes (3) - (5). The un-drifted or small shift in position of $\nu(\text{C}=\text{N})$ dismisses the possibility of coordination of azomethine nitrogen. The splitting of $\beta(\text{C}-\text{O})$ (naphtholic) band of the dihydrazone affirms the coordination through naphtholic $-\text{C}-\text{O}$ group. Further, the appearance of a medium band of $\nu(\text{N}-\text{N})$ and its un-shifted position affirms that only one hydrazinic nitrogen is

involved in bonding to the metal center. Hence, it may be suggested that the dihydrazone coordinates through NNOO donors of naphtholic oxygens and secondary nitrogens in complexes (3) - (5). Also, the new weak broad band between $2350\text{-}1850 \text{ cm}^{-1}$ in these three complexes may be attributed to $(\text{C}-\text{H})$ modes of vibration and overtones of aromatic ring in the picolines³⁵.

On examining the spectra of complexes (1) - (7) below 600 cm^{-1} , two new weak bands in the region $512\text{-}582 \text{ cm}^{-1}$ are observed which is assigned to $\nu(\text{M}-\text{O})$ (naphtholic) that indicates π -electron density flow of aromatic ring to the metal center through one of the naphtholic oxygen atom^{11,24,29,31}. This is also corroborated by the fact that the band at 1538 cm^{-1} due to $\nu(\text{amide II}) + \nu(\text{C}-\text{O})$ (naphtholic) is stronger in feature as compared to that in the free ligand.

The appearance of new medium, weak or strong band(s) in the complexes (2)-(7) in the region $616\text{-}699 \text{ cm}^{-1}$ may be attributed to the in-plane ring deformation due to pyridine bases signifying their coordination to the manganese center^{11,24,29,31}. The strong broad band centered at 3432 and 3449 cm^{-1} in complexes (2)-(5) is assignable to the presence of water molecules present in lattice while in the complex (1), the broad band centered at 3435 cm^{-1} is attributed to the existence of both lattice and coordinated water molecules¹¹.

The far IR spectrum of naphH_4 and complex (3) were studied in the region between $700\text{-}50 \text{ cm}^{-1}$ as a representative sample. The complex (3) showed weak intensity bands in the range below 500 cm^{-1} . A new weak band at 426 cm^{-1} and a couple of weak intensity bands at 311 and 314 cm^{-1} may be assigned to $\nu(\text{C}-\text{O})_{\text{enolate}}$ and $\nu(\text{M}-\text{N})_{\text{azomethine}}$ respectively^{11,24,29,31}. The weak intensity band at 263 cm^{-1} may be assigned to $\nu(\text{M}-\text{N})_{\text{pic}}$ ^{11,24,29,31}.

Cyclic voltammetry: The cyclic voltammograms of 2 mmol solutions of the ligand and complexes (1) and (3) in DMSO under nitrogen were carried out as representative cases using 0.1 M TBAP as a supporting electrolyte. The data have been set out in table 5 at a scan rate of 100 mV/s. The voltammograms were recorded within the potential range of +1.5 V to -1.5 V. The free ligand exhibited redox activity with irreversible cathodic and anodic peaks at potentials -0.4604V and +0.8802 V, respectively. The complexes (1) and (3) exhibited almost similar voltammograms with no shift or small shift of the irreversible cathodic peak potentials and a small shift of the irreversible anodic peaks towards lower potential. Hence, both these cathodic and anodic peaks in complexes (1) and (3) are suggested to be ligand-based. The current intensity of the ligand-based cathodic peaks at -0.4551 and -0.4604 V appears to be increased in complexes (1) and (3), respectively. Correspondingly, such features indicate changes due to overlap of the metal-associated cathodic peak with that of the uncoordinated dihydrazone. Besides these, a new additional anodic peak potential at -0.2405 V in the complex (1) and -0.3125 V in the case of complex (3) was observed.

The electrochemical reversibility of the redox couple at -0.35 V ($E_{1/2}$) ($\Delta E = 214$ mV) for the complex (1) and -0.39V ($E_{1/2}$) ($\Delta E = 148$ mV) for complex (3) against Ag/AgCl electrode indicates the process is quasi-reversible. The features of these redox couples in both complexes indicate the existence of Mn(IV)/Mn(III) transition-based redox activity. The decrease in oxidation potential in going from the complex (1) to (3) indicates the ease in removal of electron density towards the metal due to the incorporation of the N-donor base (methyl pyridine) in the complex (3)¹¹.

Antibacterial study: A clear zone of inhibition is observed near agar well in the plates when the samples of ligand and complexes limited the growth of the microorganisms that indicated their activities²⁵. The results obtained from the measurement of the observed zone of inhibition for the tested different bacterial species are tabulated in table 6. Evaluation of this table showed that the inhibition zone of 6-8 mm observed for naphH₄ against *Staphylococcus epidermis* (MTCC 435), *Enterobacter aerogenes* (MTCC

8559) and *Proteus vulgaris* (MTCC 426) indicated its modest activity while it is found to be highly active against *Escherichia coli* (MTCC 1669) with an inhibition zone of 10 mm. The metal complexes (1)-(5) that were screened for antibacterial activity showed the zone of inhibition values in the range 4-25 mm, thus exhibiting higher activity against both the gram-positive and gram-negative bacteria than the uncoordinated ligand.

It was noted that these complexes exhibited the highest potent activity against gram-negative bacteria *Enterobacter aerogenes* (MTCC 8559) with inhibition zones in the range of 14-25 mm. Notably, with the incorporation of axial monodentate secondary ligands, the complexes (2) - (5) showed an increased potency of bioactivity more than the complex (1) without a pyridine base.

Examination of table 6 reveals that the activity of Schiff base ligand has increased on complexation with the metal which is in good agreement with the reports on the enhancement of antibacterial activities due to Tweedy's chelation effect^{4,19}. Studies have shown that the presence of amido, azomethine^{3,15} and pyridine⁵ moieties as structural components enhances the bactericidal activity.

It is worthy to mention here that most gram-negative bacteria are known to be resistant to antimicrobial agents, hence, these microorganisms are difficult to treat^{14,20}. As reported by Abdallah *et al*¹, the antibiotics that affect the gram-negative bacteria may have potency as antitumour drugs since researchers working in the field of antitumours consider antimicrobial activity against the gram-negative bacteria for preliminary tests. Hence, these manganese(IV) complexes might be considered good in line for investigation on their antitumour activity and therefore would need to be further studied.

Conclusion

The study documents the formation of Mn(IV) complexes under a set of experimental conditions where aerial oxidation of Mn(II) to Mn(IV) has occurred. The redox-active and deprotonated electron-rich ligand naphH₄ was able to stabilize the high oxidation state (+4) of manganese.

Table 5
Electrochemical data for the ligand and its manganese(IV) complexes (Pot. vs Ag/AgCl)
at a scan rate of 100 mV/s

Ligand/Complex	Cathodic Peak Potential, $E_{pc}(V)$	Anodic Peak Potential $E_{pa}(V)$
naphH ₄	-0.4604 -	- +0.8802
[Mn ^{IV} (naph)(H ₂ O) ₂].2H ₂ O (1)	-0.4551 -	-0.2405 +0.8496
[Mn ^{IV} (naph)(2-pic) ₂].2H ₂ O (3)	-0.4604 -	-0.3125 +0.8442

Table 6
Antimicrobial studies of ligand and its monometallic manganese(IV) complexes

Schiff base / complexes	Zone of inhibition(mm)						
	Gram-positive			Gram-negative			
	<i>Staphylococcus epidermis</i>	<i>Bacillus cereus</i>		<i>Klebsiella pneumonia</i>	<i>Escherichia coli</i>	<i>Enterobacter aerogenes</i>	<i>Proteus vulgaris</i>
Ligand	08 ⁺⁺	-		-	10 ⁺⁺⁺	06 ⁺⁺	08 ⁺⁺⁺
1	12 ⁺⁺⁺	08 ⁺⁺		10 ⁺⁺⁺	-	14 ⁺⁺⁺	08 ⁺⁺⁺
2	10 ⁺⁺⁺	12 ⁺⁺		12 ⁺⁺⁺	-	22 ⁺⁺⁺	08 ⁺⁺⁺
3	-	-		06 ⁺⁺	-	25 ⁺⁺⁺	10 ⁺⁺⁺
4	-	06 ⁺⁺		20 ⁺⁺	04 ⁺	18 ⁺⁺⁺	-
5	12 ⁺⁺⁺	20 ⁺⁺⁺		20 ⁺⁺⁺	20 ⁺⁺⁺	22 ⁺⁺⁺	18 ⁺⁺⁺

Highly active = +++ (inhibition zone > 8.2mm); moderately active = ++ (inhibition zone > 5.0- 8.2); slightly active = + (inhibition zone > 2.5-5.0 mm); Inactive = - (inhibition zone < 2.5mm)

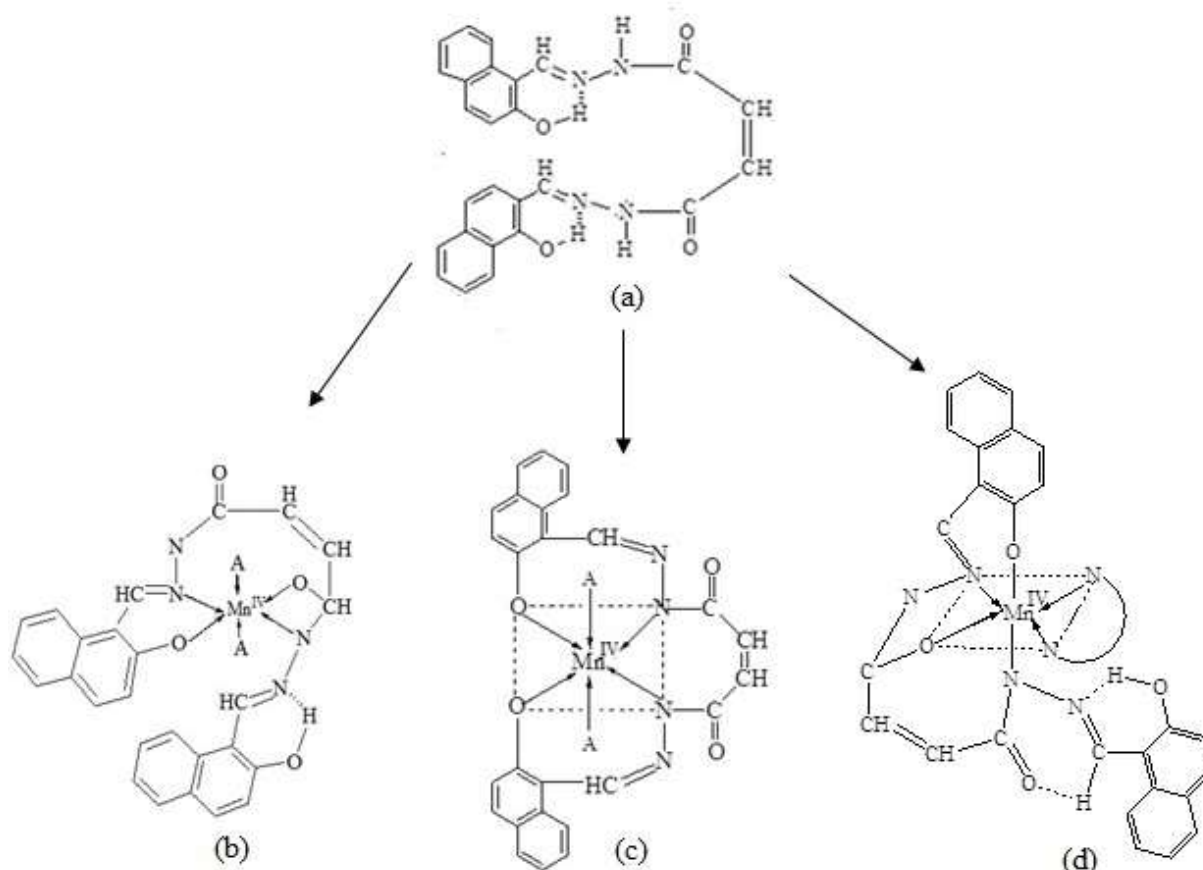


Fig. 2: Schematic drawings of (a) Ligand (napfh) (b) Complex $[\text{Mn}^{\text{IV}}(\text{napfh})(\text{A})_2] \cdot 2\text{H}_2\text{O}$ (where A = H_2O , (1); py, (2)) (c) Complex $[\text{Mn}^{\text{IV}}(\text{napfh})(\text{A})_2] \cdot 2\text{H}_2\text{O}$ (where A = 2-pic, (3); 3-pic, (4); 4-pic(5) and (d) Complex $[\text{Mn}^{\text{IV}}(\text{napfh})(\text{NN})]$ (where NN = bpy, (6); 1, 10-phen, (7))

As inferred from the IR spectra, the dihydrazone is present in a keto-enol form in complexes (1), (2), (6) and (7) while it exists in keto form in complexes (3) - (5). The dihydrazone functions as a tetradentate ligand and incorporates NNOO donors to coordinate $\text{Mn}(\text{IV})$ ion. In complexes (1), (2), (6) and (7), the binding is through a naphtholate oxygen and azomethine nitrogen of one hydrazone arm and enolate and secondary nitrogen of the other hydrazone moiety. Meanwhile, in complexes (3)-(5), the coordination is through the naphtholate oxygens and secondary nitrogens.

In complexes (1)-(5), two monodentate secondary ligands such as H_2O (1)/py(2)/2-pic(3)/3-pic(4) or 4-pic(5) occupy the axial positions while in complexes (6) and (7), a single bidentate secondary ligand (bpy(6)/phen(7)) occupies the equatorial positions. The concurrent bonding through the NNOO tetradentate donors of dihydrazone and monodentate (O/N donors) or bidentate (N-donors) of secondary ligands to the same metal center introduces steric crowding, hence, one hydrazone arm remains in the equatorial plane while the other hydrazone arm is axial. In such configurations, the

axial azomethine absorbs at a lower frequency than the equatorial azomethine as predicted from the presence of a couple of $\nu(\text{C}=\text{N})$ bands in IR spectra of all the complexes and splitting of the $\beta(\text{C}-\text{O})$ (naphtholic) bands in complexes (1)-(5). Such features in IR spectra have also been reported in many previous metal complexes of dihydrazones^{11,29,30}. Thus, the ligand is suggested to be coordinated to manganese in an anti-cis configuration.

The magnetic susceptibility data in all cases support the electronic and EPR data suggesting that the Mn(IV) ion is in octahedral stereochemistry in the complexes. The dihydrazone is electroactive and the redox potentials in the complexes (1) and (3) are consistent with the ligand as well as metal-centered Mn(IV)/Mn(III) redox activity.

The antibacterial studies on complexes (1) - (5) suggested a good antibacterial activity towards both gram-positive and gram-negative bacteria. Also, it is noticeable that incorporation of the axial monodentate secondary ligands in complexes (2) - (5) showed increased bioactivity, more than complex (1) without a pyridine base. Here, it is worth mentioning that most gram-negative bacteria are seemed as difficult to be treated when inferred in terms of their relation to barrier function of the envelope^{1,20}.

On the assessment of various analytical and spectral investigations, the tentative structures for the complexes were proposed that are presented as a schematic diagram in fig. 2.

Acknowledgement

The authors PM and PS are thankful to MHRD, Govt. of India for RA offered under the TEQIP-III project.

References

1. Abdallah M.S., Zayed M.A. and Mohamed G.G., Synthesis and spectroscopic characterization of new tetradentate Schiff base and its coordination compounds of NOON donor atoms and their antibacterial and antifungal activity, *Arabian J. Chem.*, **3**, 103 (2010)
2. Adhikari S., Lal R.A., Debnath A. and Dey D., Synthesis and characterization of Manganese (IV) complexes of polyfunctional dihydrazones containing amide, azomethane and phenol functions, *J. Chem. Pharm. Res.*, **9**, 236 (2017)
3. Ahmed A.H., Hassan A.M., Gumaa H.A., Mohamed B.H. and Eraky A.M., Mn²⁺-complexes of N, O-dihydrazone: Structural studies, indirect band gap energy and corrosion inhibition on aluminum in acidic medium, *J. Chil. Chem. Soc.*, **4**, 63 (2018)
4. Bakare S.B., Cu(II), Co(II), Ni(II), Mn(II) and Zn(II) Schiff base complexes of 3-hydroxy-4-[N-(2-hydroxynaphthylidene)-amino]-naphthalene-1-sulfonic acid: Synthesis, spectroscopic, thermal and antimicrobial studies, *Pol. J. Chem. Tech.*, **3**, 21 (2019)
5. Chaudhary N.K. and Mishra P., Metal complexes of a novel Schiff base based on penicillin: Characterization, molecular modeling and antibacterial activity study, *Bioinorg. Chem. Appl.*, DOI:10.1155/2017/6927675 (2017)
6. Costa R.O., Ferreira S.S., Pereira C.A., Harmer J.R., Noble C.J., Schenk G., Franco R.W.A., Resende J.A.L.C., Comba P., Roberts A.E., Fernandes C. and Horn A.Jr., A new mixed-valence Mn(II)Mn(III) compound with catalase and superoxide dismutase activities, *Frontiers Chem.*, **6**, 491 (2018)
7. Geary W.J., The use of conductivity measurements in organic solvents for the characterisation of coordination compounds, *Coord. Chem. Rev.*, **7**, 81 (1971)
8. Gutierrez K., Corchado J., Lin S., Chen Z. and Cruz D.M.P., A non-innocent salen naphthalene ligand and its Co²⁺, Ni²⁺ and Cu²⁺ metal complexes: Structural, electrochemical and spectroscopic characterization and computational studies, *Inorg. Chim. Acta*, **474**, 118 (2018)
9. Karaböcek S. and Karaböcek N., Mono- and dinuclear copper(II) complexes of a Schiff base ligand, 4',5'- bis(salicylideneimino)-benzo-15-crown-5, *Polyhedron*, **16**, 1771 (1997)
10. Kessissoglou D.P., Li X., Butler W.M. and Pecoraro V.L., Mononuclear manganese(IV) complexes of hydroxyl-rich Schiff base ligands, *Inorg. Chem.*, **26**, 2487 (1987)
11. Lal R.A., Basumatary D., Chanu O.B., Lemtur A., Asthana M., Kumar A. and De. A.K., Synthesis, characterization, reactivity and electrochemical studies of manganese(IV) complexes of bis(2-hydroxy-1-naphthaldehyde)adipoyldihydrazone, *J. Coord. Chem.*, **64**, 300 (2011)
12. Lal R.A., Adhikari S., Kumar A., Chakraborty J. and Bhaumik S., Synthesis and characterization of manganese(IV) complexes derived from the direct reaction of manganese(II) acetate tetrahydrate with oxaloyldihydrazide and 2-hydroxy-1-naphthaldehyde, *Synth. React. Inorg. Met.-Org. Chem.*, **32**, 81 (2002)
13. Mani B., Natarajan S., Ha H., Lee Y.H. and Nam K.T., Involvement of high-valent manganese-oxo intermediates in oxidation reaction: realisation in nature, nano and molecular systems, *Nano Convergence*, **5**, 18 (2018)
14. Matshwele J.T.P., Nareetsile F., Mapolelo D., Matshameko P., Leteane M., Nkwe D.O. and Odisitse S., Synthesis of mixed ligand Ruthenium (II/III) complexes and their antibacterial evaluation on drug-resistant bacterial organisms, *J. Chem.*, DOI:10.1155/2020/2150419 (2020)
15. Mohammed M.A.N., Synthesis and characterization of bis-acylhydrazone derivatives as tetradentate ligands and their dinuclear metal(II) complexes, *Periodica Polytechnica*, **56**, 83 (2012)
16. Mukhopadhyay R., Bhattacharjee S. and Bhattacharyya R., Ligand control on the synthesis and redox aspects of mononuclear manganese-(III) and -(IV) complexes with tridentate ONS-coordination, *Proc. Indian Acad. Sci. (Chem. Sci.)*, **108**, 193 (1996)
17. Murukan B. and Kochukittan M., Synthesis, characterization and antibacterial properties of some trivalent metal complexes with [(2-hydroxy-1-naphthaldehyde)-3-isatin]-bishydrazone, *J. of Enzyme Inhibition and Medicinal Chem.*, **22**, 65 (2007)

18. Najafpour M.M., Moghaddam A.N., Allakhverdiev S.I. and Govindjee, Biological water oxidation: Lessons from nature, *Biochimica et Biophysica Acta*, **1817**, 1110 (2012)
19. Neelakantan M.A., Esakkiammal M., Mariappan S.S., Dharmaraja J. and Jeyakumar T., Synthesis, characterization and biocidal activities of some Schiff base metal complexes, *Indian J. Pharm. Sci.*, **72**, 216 (2010)
20. Nikaido H. and Nakae T., The outer membrane of gram-negative bacteria, *Adv. Microbiol. Physiol.*, **20**, 163 (1979)
21. Okawa H., Nakamura M. and Kida S., Binuclear metal complexes, XLII, Manganese(IV) complexes synthesized by oxidation of binuclear manganese(II) complexes of 2-(salicylidene-amino) phenols with tetrachloro-o-benzoquinone, *Bull. Chem. Soc. Japan*, **55**, 466 (1982)
22. Pass G. and Sutcliffe H., The preparation of some manganese compounds, In *Practical Inorganic Chemistry*, Springer, Dordrecht (1974)
23. Pradeep C.P., Zacharias P.S. and Das S.K., A chiral Mn(IV) complex and its supramolecular assembly: Synthesis, characterization and properties, *J. Chem. Sci.*, **118**, 311 (2006)
24. Refat M.S., El-Korashy S.A., Kumar D.N. and Ahmed S.A., Syntheses and characterization of Ru(III) with chelating containing ONNO donor quadridentate Schiff bases, *Spectrochim. Acta*, Part A, **70**, 898 (2008)
25. Reller L.B., Weinstein M., Jorgensen J.H. and Ferraro M.J., Antimicrobial susceptibility testing: A review of general principles and contemporary practices, *Clin. Infect. Dis.*, **49**, 1749 (2009)
26. Sadhukhan D., Ray A., Pilet G., Rosair G.M., Garribba E., Nonat A., Charbonnière L.J. and Mitra S., Cobalt(II), manganese(IV) mononuclear and zinc(II) symmetric dinuclear complexes of an aliphatic hydrazone Schiff base ligand with diversity in coordination behaviors and supramolecular architectures: Syntheses, structural elucidations, and spectroscopic characterizations, *Bull. Chem. Soc. Jpn.*, **84**, 764 (2011)
27. Sarkar N., Harms K., Frontera A. and Chattopadhyay S., Importance of C–H... π interactions in stabilizing the *syn/anti* arrangement of pendant alkoxy side arms in two manganese(IV) Schiff base complexes: Exploration of catechol oxidase and phenoxazinone synthase like activities, *New J. Chem.*, **41**, 8053 (2017)
28. Schreiber R.E., Cohen H., Leitun G., Wolf S.G., Zhou A., Que L.Jr. and Neumann R., Reactivity and O₂ formation by Mn(IV)- and Mn(V)-hydroxo species stabilized within a polyfluoroxometalate framework, *J. Am. Chem. Soc.*, **137**, 8738 (2015)
29. Singh M.K., Kar N.K. and Lal R.A., Synthesis and characterization of manganese(IV) and ruthenium(III) complexes derived from *bis*(2-hydroxy-1-naphthaldehyde)oxaloyldihydrazone, *J. Coord. Chem.*, **61**, 3158 (2008)
30. Singh M.K., Kar N.K. and Lal R.A., Synthesis and structural characterization of manganese(III, IV) and ruthenium(III) complexes derived from 2-hydroxy-1-naphthaldehydebzoyl hydrazone, *J. Coord. Chem.*, **62**, 1677 (2009)
31. Temel H. and Şekerci M., Novel complexes of manganese(III), cobalt(II), copper(II) and zinc(II) with Schiff base derived from 1,2-bis(*p*-amino-phenoxy) ethane and salicylaldehyde, *Synth. React. Inorg. Met.-Org. Chem.*, **31**, 849 (2001)
32. Vogel A.I., *A Textbook of Quantitative Inorganic Analysis Including Elementary Instrumentation Analysis*, 4thed., London, Longmans (1978)
33. Zlatar M., Gruden M., Vassilyeva O.Y., Buvaylo E.A., Ponomarev A.N., Zvyagin S.A., Wosnitza J., Krzystek J., Fernandez P.G. and Duboc C., Origin of the zero-field splitting in mononuclear octahedral Mn^{IV} complexes: A combined experimental and theoretical investigation, *Inorg. Chem.*, **55**, 1192 (2016)
34. Zou J., Huang J., Yue D. and Zhang H., Roles of oxygen and Mn(IV) oxide in abiotic formation of humic substances by oxidative polymerization of polyphenol and amino acid, *Chemical Engineering Journal*, **393**, 124734 (2020)
35. Garza-Ortiz A., Maheswari P.U., Siegler M., Spek A.L. and Reedijk J., A new family of Ru(II) complexes with a tridentate pyridine Schiff-base ligand and bidentate co-ligands, Synthesis, characterization, structure and *in vitro* cytotoxicity studies, *New J. Chem.*, **37**, 3450 (2013).

(Received 16th December 2020, accepted 30th January 2021)